

Evaluation of Wave-induced Liquefaction in a Porous Seabed: Using an Artificial Neural Network and a Genetic Algorithm -based model

Daeho (Fred) Cha^{*}
Dong-Sheng Jeng^{**}
Michael Blumenstein^{***}
Hong Zhang^{*}

^{*}School of Engineering, Griffith University, Gold Coast Campus
Gold Coast Mail Centre, QLD, Australia

^{**}Department of Civil Engineering, The University of Sydney,
NSW, Australia

^{***}School of Information and Communication Technology, Griffith University, Gold Coast Campus
Gold Coast Mail Centre, QLD, Australia

ABSTRACT

The evaluation of wave-induced liquefaction is one of the key factors for analysing seabed characteristics and the design of marine structures. Numerous investigations of wave-induced liquefaction have been proposed. However, most previous research has focused on complicated mathematical theories and laboratory work. In this study, we contribute an alternative approach for the prediction of the wave-induced liquefaction using an Artificial Neural Network (ANN) and a Genetic Algorithm (GA)-based model. Combined ANN and GA-based models are still a newly developed area in coastal engineering. In this study, a Genetic Algorithm-based approach is proposed to find optimal weights for the ANN model. It reduces the training time, and improves the forecasting accuracy for wave-induced maximum liquefaction depth, compared to using the normal ANN training procedure. Simulation results demonstrate the capacity of the proposed ANN model for the prediction of wave induced maximum liquefaction depth in addition to the proposal of GAs for training the ANN model.

KEY WORDS: Liquefaction; artificial neural networks; genetic algorithms.

INTRODUCTION

In the last few decades, various investigations of wave-induced seabed liquefaction have been carried out. The reason for the numerous research studies focused on this topic is that vertical movement of sediment, might cause the instability of the structure. Bjerrum (1973) is possibly the first person that considered the wave-induced liquefaction occurring in saturated seabed sediments. Later, Nataraja et al. (1980) suggested a simplified procedure for ocean wave-induced

liquefaction analysis. Recently, Rahman (1991) established the relationship between liquefaction and characteristics of wave and soil. He concluded that liquefaction potential increases the degree of saturation with an increase of wave period. Jeng (1997) examined four different criteria of the wave-induced liquefied state, together with Zen and Yamazaki's (1991) field data. He also conducted a parametric study and concluded that no liquefaction occurs in a saturated seabed, except in very shallow water, large waves and seabed with very low permeability. For a more advanced poro-elastoplastic model for the wave-induced liquefaction potential, the readers can refer to Sassa and Sekiguchi (2001) and Sassa et al. (2001). All aforementioned investigations have been reviewed by Jeng (2003). In summary, all previous investigations for the wave-induced liquefaction potential in a porous seabed have been based on various assumptions of engineering mechanics, which limits the application of the model in realistic engineering problems.

Recently, ANNs have been applied to various engineering fields, such as prediction of rainfall intensity. (French *et al.*, 1992), generation of wave equations based on hydraulic data (Yonas *et al.*, 1999), tide-forecasting (Lee & Jeng, 2002), prediction of settlement of shallow foundations (Mohamed *et al.*, 2002) and modeling confinement efficiency of reinforced concrete (Tang *et al.*, 2003).

Major difference between traditional engineering mechanics approaches and ANN models for the estimation of the wave-induced liquefaction is the procedure. Conventional models for wave-induced liquefaction procedures always involve complicated mathematical calculations with numerous variables, such as shear modulus, degree of saturation and Poisson ratio *etc.* However, ANNs model can be simply built and can learn the knowledge of a database without complicated

governing equations. It only requires a reliable database, which includes input data and output data.

For the liquefaction consideration, such as the prediction of seismic liquefaction potential, back-propagation neural networks have been widely used by Goh (1995). Later, Juang and Chen (1999) predicted seismic liquefaction potential from cone penetration field test data. ANN models have been used for the liquefaction-induced horizontal ground displacement (Wang and Rahman, 1999), and lately, Jeng *et al.* (2003) predict earthquake-induced liquefaction using an ANN model. Recently, Cha *et al.* (2004) applied ANNs for the prediction of wave-induced liquefaction in a porous seabed. Their research demonstrated the capability of ANN models for the prediction of the maximum wave-induced liquefaction depth within various wave and soil conditions.

Genetic Algorithm-based models (GA) were proposed by John Holland in the 1970s (Holland, 1975), he introduced major components of GAs such as population-based algorithms with crossover, inversion, and mutation. GAs are mainly designed to solve optimization problems. However, there are scarce studies for the application of ANNs and genetic algorithms (GAs) for wave-induced seabed liquefaction. Thus, in this study, we adopt GA design for an exist ANN model for the wave-induced seabed maximum liquefaction (Cha *et al.* 2004).

Porosity-elastic Model

In this study, we consider an ocean wave propagating over a porous seabed of finite thickness. The definition of the problem is illustrated in Fig. 1. Considering a two-dimensional wave-seabed interaction problem, and treating the porous seabed as hydraulically isotropic with the same permeability. Biot (1956) presented a general set of equations governing the behaviour of a linear elastic porous solid under dynamic conditions. They are summarized in the tensor form as below

$$\sigma_{ij,j} = \rho \ddot{u}_i + \rho_f \ddot{w}_i, \quad (1)$$

$$-p_{,i} = \rho_f \ddot{u}_i + \frac{\rho_f}{n} \ddot{w}_i + \frac{\rho_f g}{k_z} \dot{w}_i, \quad (2)$$

$$\dot{u}_{i,i} + \dot{w}_{ii} = -\frac{n}{k_f} \dot{p}, \quad (3)$$

where p is pore pressure, u and w are the displacements of solid and relative displacements of solid and fluid, $1/k_f$ is the compressibility of pore fluid, which is defined by

$$\frac{1}{k_f} = \frac{1}{2 \times 10^9} + \frac{1-S}{P_{wo}} \quad (4)$$

where S is the degree of saturation, P_{wo} is the absolute water pressure.

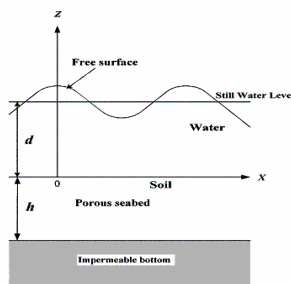


Fig.1 Definition of wave-seabed interaction.

The definition of effective stress σ'_{ij} , which is assumed to control the deformation of the soil skeleton, is given for the total stress σ_{ij} as $\sigma_{ij} = \sigma'_{ij} - \delta_{ij} p$, where δ_{ij} is the Kronecker Delta notation.

From Eq. 1 we have

$$-\left(\frac{n}{k_f} \dot{p}\right)_i = (\dot{\epsilon}_{ii} + \dot{w}_{ii})_i \quad (5)$$

Substituting Eq. 5 into Eq. 1 and Eq. 2, the governing equation can be rewritten as:

$$\frac{k_f}{n} (u_{i,i} + w_{i,i})_i = \rho_f \ddot{u}_i + \frac{\rho_f}{n} \ddot{w}_i + \frac{\rho_f g}{k_z} \dot{w}_i \quad (6)$$

$$\sigma'_{ij,j} = -\frac{k_f}{n} \delta_{ij} (u_{i,i} + w_{i,i})_i + \rho \ddot{u}_i + \rho_f \ddot{w}_i \quad (7)$$

If the acceleration terms are neglected in the above equations, it becomes the consolidation equation, which has been used in previous work (Jeng, 1997).

Since the wave-induced oscillatory soil response fluctuates periodically in the time domain, all quantities can be replaced immediately by their complex forms.

$$f = \bar{f} e^{i(kx - \omega t)} \quad (8)$$

where k is the wave number and ω is the wave frequency.

Herein, to simplify the expression of equations, we introduce three new parameters defined by

$$K_1 = G/[G/(1-2\mu) + k_f/n], \quad (9)$$

$$K_2 = [k_f/n]/[G/(1-2\mu) + k_f/n], \quad (10)$$

$$V_c^2 = [G/(1-2\mu) + k_f/n]/\rho. \quad (11)$$

Eqs. 6-7 can be expressed in scalar form as

$$K_1 D^2 \bar{U}_1 - \frac{2(1-2\mu)}{1-2\mu} K_1 \bar{U}_1 + \Pi_2 \bar{U}_1 - K_2 \bar{U}_1 + iD \bar{U}_2 + (\Pi_2 \beta - K_2) \bar{W}_1 + iKD \bar{W}_2 = 0 \quad (12)$$

$$\left[\frac{2(1-\mu)}{1-2\mu} K_1 D^2 + K_2 D^2 - K_1 + \Pi_2 \right] \bar{U}_2 + iD \bar{U}_1 + iK_2 D \bar{W}_1 + (K_2 D^2 + \Pi_2 \beta) \bar{W}_2 = 0 \quad (13)$$

$$(\beta \Pi_2 - K_2) \bar{U}_1 + iK_2 D \bar{U}_2 + \left(\frac{\beta}{n} \Pi_2 - K_2 + \frac{i}{\Pi_1} \right) \bar{W}_1 + iK_2 D \bar{W}_2 = 0 \quad (14)$$

$$iK_2 D \bar{U}_1 + [K_2 D^2 + \beta \Pi_2] \bar{U}_2 + iK_2 D \bar{W}_1 + \left[K_2 D^2 + \frac{\beta}{n} \Pi_2 + \frac{i}{\Pi_1} \right] \bar{W}_2 = 0 \quad (15)$$

where $\beta = \rho_f / \rho$, $\bar{u}_i = \bar{U}_i e^{i(\bar{x} - \bar{t})}$ and $\bar{w}_i = \bar{W}_i e^{i(\bar{x} - \bar{t})}$, and Π_1 and Π_2 are defined as

$$\Pi_1 = \frac{k_z V_c^2 k^2}{\rho_f g \omega} \quad \text{and} \quad \Pi_2 = \frac{\rho \omega^2}{\left(\frac{G}{1-2\mu} + \frac{K_f}{n} \right) k^2} \quad (16)$$

Eqs. 12~15 can be solved. The general solution of wave-induced soil and pore fluid displacement s can be expressed as

$$\bar{U}_1 = a_1 e^{\lambda_1 z} + a_2 e^{-\lambda_1 z} + a_3 e^{\lambda_2 z} + a_4 e^{-\lambda_2 z} + a_5 e^{\lambda_3 z} + a_6 e^{-\lambda_3 z} \quad (17)$$

$$\bar{U}_2 = b_1 a_1 e^{\lambda_1 z} + b_2 a_2 e^{-\lambda_1 z} + b_3 a_3 e^{\lambda_2 z} + b_4 a_4 e^{-\lambda_2 z} + b_5 a_5 e^{\lambda_3 z} + b_6 a_6 e^{-\lambda_3 z} \quad (18)$$

$$\bar{W}_1 = c_1 a_1 e^{\lambda_1 z} + c_2 a_2 e^{-\lambda_1 z} + c_3 a_3 e^{\lambda_2 z} + c_4 a_4 e^{-\lambda_2 z} + c_5 a_5 e^{\lambda_3 z} + c_6 a_6 e^{-\lambda_3 z} \quad (19)$$

$$\bar{W}_2 = d_1 a_1 e^{\lambda_1 z} + d_2 a_2 e^{-\lambda_1 z} + d_3 a_3 e^{\lambda_2 z} + d_4 a_4 e^{-\lambda_2 z} + d_5 a_5 e^{\lambda_3 z} + d_6 a_6 e^{-\lambda_3 z} \quad (20)$$

where, λ_i coefficients are the roots of the characteristics equation, form the equations. The b_i , c_i and d_i coefficients can be derived from Eqs. 12~15.

Based on the wave-induced soil and fluid displacements, we can obtain the wave-induced pore pressure, effective stresses and shear stresses. The six unknown coefficients, a_i ($i=1\sim 6$) can be solved. Once we obtain the a_i coefficients, we can calculate the wave-induced soil response parameters. Detailed information of the above solution can be found in Jeng and Cha (2003).

Wave-induced Liquefaction

It has generally been accepted that when the vertical effective stress vanishes. The soil will be liquefied. Thus, the soil matrix loses its strength to carry and load and consequently causes seabed instability. Based on the concept of excess pore pressure, Zen and Yamazaki (1990) proposed a criterion of liquefaction, which has been further extended by considering the effects of lateral loading (Jeng, 1997)

$$-\frac{1}{3}(1+2K_o)(\gamma_s - \gamma_w)z + (P_b - p) \leq 0 \quad (21)$$

where K_o is the coefficient of earth pressure at rest, which is normally varied from 0.4 to 1.0, and 0.5 is commonly used for marine sediments (Scott, 1968). In Eq. 21, γ_s is the unit weight of soil, γ_w is the unit weight of water, and P_b is the wave pressure at the seabed surface, which is given by

$$P_b(x, t) = \frac{\gamma_w H}{2 \cosh kd} \cos(kx - \omega t) \quad (22)$$

where, H is the wave height and d is the water depth.

Artificial Neural Networks

ANNs were originally based on the biological brain, whereby the basic idea is that they model the simplest brain functions. A basic artificial neuron is shown in Fig. 2.

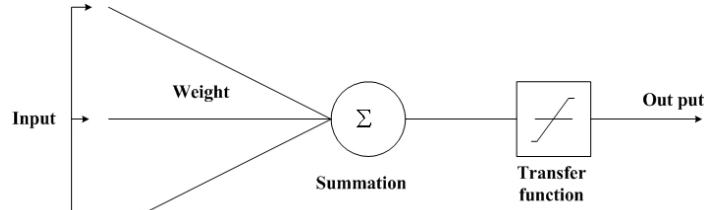


Fig.2 Basic representation of an artificial neuron

In an ANN model (as seen in Fig. 3), each layer is built by several neurons and the layers are interconnected by sets of weights. The input layer neurons receive initial input information, after that outputs are produced by a transformation using various transfer functions. In this paper we adopted the log-sigmoid transfer function, which is shown in Eq. 23.

$$f(x) = \frac{1}{1 + e^{-x}} \quad (23)$$

In the learning procedure, the interconnection weights are adjusted using the relationships between input and output values, which is an important part of the ANN model. There are various types of ANN training algorithms that may employed to adjust these weights. The back-propagation algorithm is one of the most representatives for training artificial neural networks for various applications. The back-propagation algorithm uses the gradient steepest descent procedure to determine the weights of inter-connected neurons. The gradient descent method is utilised to calculate the weights of the network and to adjust them to minimise the output error. It can be applied to networks, which have at least one hidden layer, and are fully connected to all units in each layer. The main procedure of the back-propagation algorithm is that the error at the output layer is iteratively propagated backwards to the input layer through the hidden layer in the network to modify the weights and obtain the final desired outputs. Thus, the goal of this procedure is to obtain a desired output when certain inputs are given. The functionality described results in a network architecture as shown in Fig. 3. The error function, which is used in this paper, is shown in Eq. 24, where D_i and O_i are respectively the desired and actual output values. M is the total number of training data set. Since the error is the difference between the actual output and the desired output, the error depends on the weights, and we need to adjust the weight in order to minimize the error. We can hence adjust the weights using the method of gradient descent as described above. The details of back-propagation training algorithm can be found in Rumelhart *et al.* (1986).

$$E = \frac{1}{M} \sum_{i=1}^M (D_i - O_i)^2 \quad (24)$$

In this study, we establish the ANN model using Matlab's Neural Network Toolbox, which provides an effective way for programming.

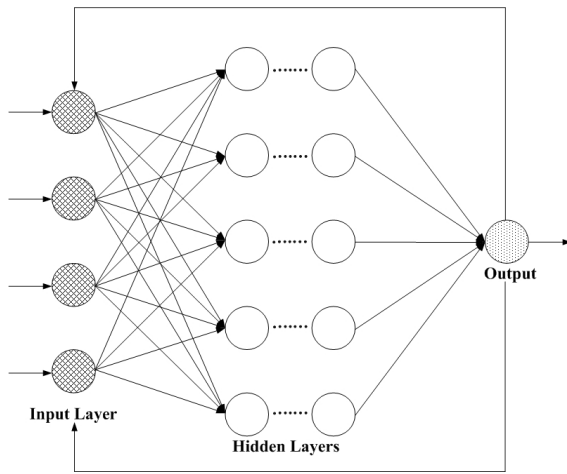


Fig.3 Typical multi-layered neural network model

Numerical Simulations

The performance of the ANN depends on the number of hidden layers, the learning factors, the training iteration (epoch) numbers, the weights and the number of neurons in each layer. These factors, for this study, are displayed in Table 1.

Table 1. Input factors for ANN model.

Training model	
Number of input Neurons	5
Number of Output Neurons	1
Number of Hidden units	4
Learning rate	0.5
Momentum factor	0.2
Epochs	9000

The input data for the poro-elastic model, which establishes the ANN model, are shown in Table 2. As seen in the table, we built the database, based on the most possible ranges of wave and soil conditions. As the test indicates, liquefaction occurs in numerous cases.

In the case study, we had approximately 15,000 data items for maximum liquefaction depth from each numerical model. Among this data we used 80% for the training procedure, and the remaining data was used for testing the prediction capability.

Table 2. Input data for the poro-elastic model

Soil Characteristics	
Soil permeability (k_z)	10^{-4} (m/sec)
Seabed thickness (h)	10m or variation
Shear modulus (G)	10^7 N/m ²
Poisson ratio (μ)	0.4
Porosity (n)	0.35
Degree of saturation (S)	0.95 or variation
Wave Characteristics	
Wave period (T)	8.00 sec variation
Wave height (H)	7.5 m or variation
Water depth (d)	50m or variation

Single-artificial neural network model (SANN) The test results for prediction of the maximum liquefaction depth and the training procedure using the proposed SANN model (Cha *et al.*, 2004) are presented in Fig. 5. Fig. 5(a) illustrates the convergence of the training procedure. It is clearly shown that the training error is less than 10^{-3} , which is based on Eq. 24. It implies that the SANN weight configuration can be used to forecast the maximum liquefaction depth with a good accuracy. Fig. 5(b) represents the prediction of the maximum liquefaction depth (Z_L) using the ANN model versus the poro-elastic numerical maximum liquefaction depth (Z_L). As seen in this figure, the prediction of maximum liquefaction agrees with the numerical calculation data overall. However, as shown in Figure 5, there is significant disagreement between the SANN model and the original database near the origin (i.e., no liquefaction). This implies that a single-network model may not be able to predict the maximum liquefaction depth if it is either small or zero.

RESULTS

Application of ANN Models for Wave-induced Liquefaction

Generally, wave-induced seabed liquefaction is predicted from complicated mathematical equations. However, the ANN model is data driven model, one of the advantages of ANN models is that appropriate input data and accurate values for the desired output data are needed. The configuration of the ANN model used in this study is shown in Fig. 4.

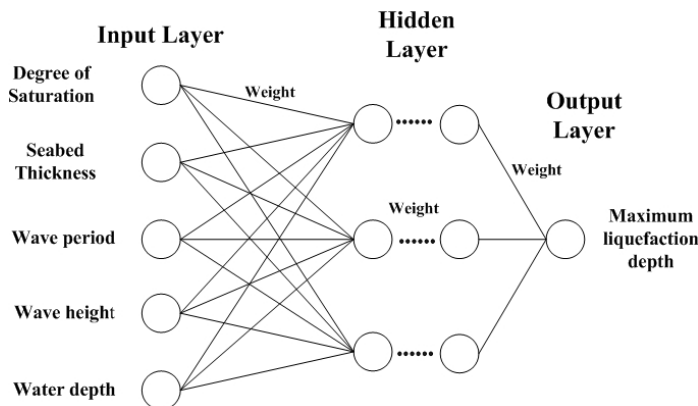
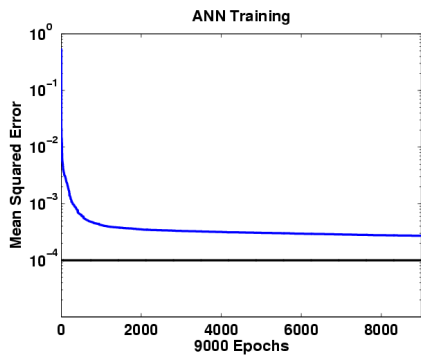
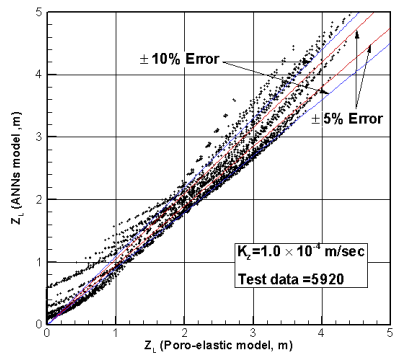


Fig. 4 Structure of ANN model for wave-induced liquefaction.

As pointed out in previous work (Jeng, 1997), the most important factors, which significantly affect the wave-induced soil liquefaction, are the degree of saturation, seabed thickness, wave period, water depth, wave height and soil permeability. Since permeability has been very sensitive to the occurrence of the wave-induced liquefaction potential, we use the other parameters as the input parameters for the ANN model with a fixed value of permeability and the wave-induced maximum liquefaction depth is used as the model's output (Fig. 4). Thus, in this study, we have one ANN model for each case, with a fixed value of soil permeability. Also, to facilitate appropriate ANN training, we normalised the input and output values between 0 and 1 by a reference value.

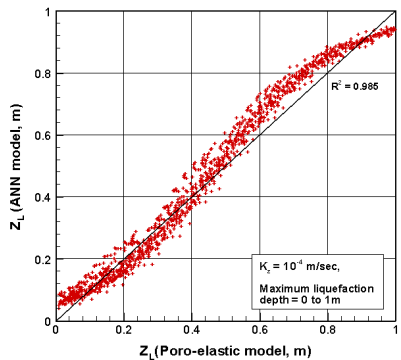


(a) Convergence of training data

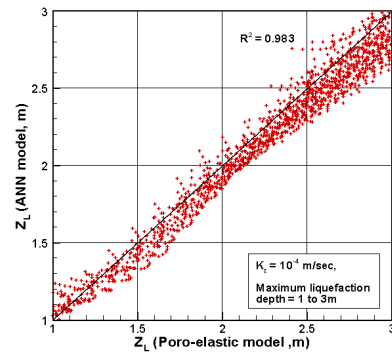


(b) Prediction of maximum liquefaction depth for the SANN model versus the poro-elastic model

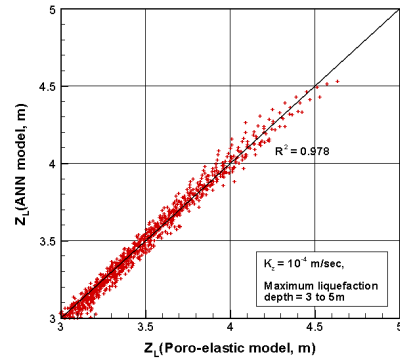
Fig. 5: (a) Convergence of training data and (b) comparison of the wave-induced maximum liquefaction depth by the SANN model versus the poro-elastic model ($K_z = 10^{-4}$ m/sec).



(a) Prediction of maximum liquefaction depth for the SANN model versus the poro-elastic model between 0 to 1m



(b) Prediction of maximum liquefaction depth for the SANN model versus the poro-elastic model between 1 to 3m



(c) Prediction of maximum liquefaction depth for the SANN model versus the poro-elastic model between 3 to 5m

Fig. 6 Comparison of the wave-induced maximum liquefaction depth by the MANN model versus poro-elastic model ($K_z = 10^{-4}$ m/sec)

Multi-artificial neural network model (MANN) The occurrence of wave-induced liquefaction depends on soil and wave parameters. However, as shown in Fig. 5, the SANN model fails to predict values near the zero liquefaction and over 3 m liquefaction depth range. Therefore, the MANN model is applied to deal with three different ranges, from 0 to 1 m, 1 to 3 m and 3 to 5 m, with three different networks. It has a similar training procedure to the SANN model, but the data used for training is divided into 3 different training databases. Fig. 6 clearly shows that each range of maximum liquefaction depth of the MANN-predicted results agree with the numerical calculation depths. It is obvious that maximum liquefaction depth ranges between 0 to 1 m and 3 to 5 m have better agreement.

Fig 6 represent the predicted maximum liquefaction depth (Z_L) using an ANN model versus (Z_L) a poro-elastic numerical maximum liquefaction depth (Z_L). As seen in the figures, the prediction of maximum liquefaction overall agrees with the numerical calculation data. It is shown that the correlation of the ANN model and the poro-elastic model is over 97%. These figures illustrate that most of prediction maximum liquefaction depths are between $\pm 10\%$ range, which is acceptable for an engineering application. The poro-elastic, numerical maximum liquefaction depth of 0m, depends on soil and wave parameters, however the ANN model predicts between 0 and 1m based on the weights of each layer and the output value.

Genetic Algorithms

The GA's main role is numerical optimisation inspired by natural evolution. GAs are capable of being applied to an extremely wide range of problems. John Holland (1975) may be the first to attempt to put computational evolution on a firm theoretical footing. A GA operates on a population of chromosomes, which are produced from crossover and mutation operations.

Application of GAs to ANN models Generally, it is time-consuming to configure and adjust the settings of an ANN model during the supervised training procedure. Even though its results are acceptable from the engineering view, an ANN model trained using GAs can reduce the complexity of the procedure; hence, it is an advantage to use them in conjunction with ANNs. The configuration of the ANN model using GAs is shown in Fig 7.

As discussed in the previous sections, ANN models predict data, based on the relationship between input and output values. This relationship is based on the iterative modification of network weights, from the training procedure. It clearly shows that the training procedure is key factor of an ANN model. However, the authors found that the training procedure can be time consuming in terms of selecting the most appropriate settings for ANN training; therefore the authors propose to use GAs to optimise the existing ANN model's weights.

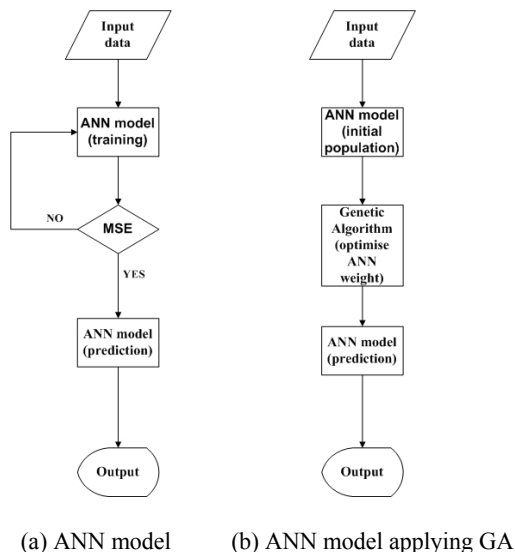


Fig.7 Comparison of an ANN model and an ANN model using GAs

Fig.7 illustrates a comparison of a standard ANN model and an ANN model trained using GAs. As may be seen in the above flow chart, an ANN model applying GAs can produce an output without repeating the training procedure: this is because there are fewer requirements to modify certain training parameters (Fig. 7(b)). We can get the initial population for the GA from the first or second epoch of the ANN training procedure. We adopted this initial population, which is the ANN's weight configuration and evaluated it through the GA's fitness function for optimisation. After the completion of the GA operation, optimised ANN weights may be produced and it can be used in an ANN model for prediction.

CONCLUSIONS

In this study, we introduced various ANN models for the prediction of the wave-induced liquefaction potential in a porous seabed. Unlike the conventional engineering mechanics approaches, the ANN model does not require a complicated mathematical procedure. We adopted the back-propagation algorithm for neural network training to forecast the maximum liquefaction depth.

Also, we adopted the concept of GA-based training of the existing ANN models to dramatically reduce the ANN training procedures without corrupting the maximum liquefaction prediction results.

ACKNOWLEDGEMENTS: The authors are grateful for the support of Griffith University Research and Development Grants (GURG2004).

REFERENCES

- Biot, MA (1956). "Theory of propagation of elastic waves in a fluid-saturated porous solid. Part I: Low frequency range; Part II. High frequency analysis," *Journal of Acoustics Society*, Vol 28, pp168-191.
- Bjerrum, J (1973). "Geotechnical problem involved in foundations of structures in the North Sea," *Geotechnique*, Vol 23, No 3, pp 319-358.
- Cha, DH (2003). "Mechanism of Ocean Waves Propagating over a Porous Seabed," *MPhil Thesis*, Griffith University, Australia.
- Cha, DH, Jeng, DS, and Blumenstein, M (2004). "Assessment of wave-induced liquefaction in a porous seabed: Application of an ANN model," *Asian Journal of Information Technology*, Vol 3, No 5, pp 375-385.
- French, NM, Witol, F, Krajewski, FW, and Cuykendallb, RR (1992). "Rainfall forecasting in space and time using a neural network," *Journal of Hydrology*, Vol 137, pp 1-31.
- Goh, ATC (1995). "Seismic liquefaction potential assessed by neural networks," *Journal of Geotechnical Engineering*, ASCE, Vol 120, No 9, pp 1467-1480.
- Holland, JH (1975). "Adaptation in Natural and Artificial Systems," *University of Michigan Press*. (Second edition:MIT Press, 1999)
- Jeng, DS (1997). "Wave-induced seabed instability in front of a breakwater," *Ocean Engineering*, Vol 24, No 10, pp 887-917.
- Jeng, DS (2003). "Wave-induced seafloor dynamics," *Applied Mechanics Review*, Vol 56, No 4, pp 407-429.
- Jeng DS, and Cha, DH (2003). "Effects of dynamic soil behaviour and wave non-linearity on the wave-induced pore pressure and effective stresses in porous seabed," *Ocean Engineering*, Vol 30, No 16, pp 2065-2089.
- Jeng, DS, Lee, TL, and Lin, C (2003). "Application of artificial neural networks in assessment of Chi-Chi earthquake-induced liquefaction," *Asian Journal of Information Technology*, Vol 2, No 3, pp190-198.
- Juang, CH, and Chen, CJ (1999). "CPT-based liquefaction evaluation using neural network," *Journal of Computer-Aided Civil Infrastructure Engineering*, Vol 14, pp 221-229.
- Lee TL, Jeng DS (2002). "Application of artificial neural networks in tide-forecasting," *Ocean Engineering*, Vol 29, pp 1003-1022.
- Maier, HR, and Dandy, GC (1996). "The use of artificial neural networks for the prediction of water quality parameters," *Water Resources Research*, Vol 32, No 4, pp 1013-1022.

- Mohamed AS, Mailer, HR, and Jaksa, MB (2002). "Predicting settlement of shallow foundations using neural networks," *Journal of Geotechnical and Geoenvironmental Engineering*, ASCE, Vol 128, pp 785-793.
- Nataraja, MS, Singh, H, Maloney, D (1980). "Ocean wave-induced liquefaction analysis: a simplified procedure," *In: Proceedings of an International Symposium on Soils under Cyclic and Transient Loadings*, pp 509-516.
- Rahman, MS (1991). "Wave-induced instability of seabed: Mechanism and conditions," *Marine Geotechnology*, Vol 10, pp 277-299.
- Rumelhart, DE, Hinton, GE, and Williams, RJ (1986). "Learning representations by back-propagating errors," *Nature* Vol 323 pp 533-536.
- Sassa, S, and Sekiguchi, H (2001). "Analysis of wave-induced liquefaction of sand beds," *Geotechnique*, Vol 51, No 2, pp 115-126.
- Sassa, S, Sekiguchi, H, and Miyamoto, J (2001). "Analysis of progressive liquefaction as moving-boundary problem," *Geotechnique*, Vol 51, No 10, pp 847-857.
- Scott, RF (1968). "Principle of Soil Mechanics," *Addison-Publishing, Massachusetts*.
- Tang, CW, Chen, HJ, and Yen T (2003). "Modeling confinement efficiency of reinforced concrete columns with rectilinear transverse steel using artificial neural networks," *Journal of Structural Engineering*, ASCE, Vol 129, pp 775-783.
- Wang, J, and Rahman, MS (1999). "A neural network model for liquefaction-induced horizontal ground displacement," *Soil Dynamics and Earthquake Engineering*, Vol 18, No 8, pp 555-568.
- Yonas B, Dibike, AWM, and Abbott, MB (1999). "Applications of artificial neural networks to the generation of wave equations from hydraulic data," *Journal of Hydraulic Research*, Vol 37, No 1, pp 81-97.
- Zen, K, and Yamazaki, H (1990). "Mechanism of wave-induced liquefaction and densification in seabed," *Soil and Foundations*, Vol 30, No 4, pp 90-104.